



Published in final edited form as:

*Osteoarthritis Cartilage*. 2012 February ; 20(2): 69–78. doi:10.1016/j.joca.2011.11.003.

## MRI of Weight-bearing and Movement

Lauren M. Shapiro<sup>1</sup> and Garry E. Gold<sup>1,2,3</sup>

<sup>1</sup>Department of Radiology, Grant Building Room S068B, Stanford, CA 94305

<sup>2</sup>Department of Bioengineering, Grant Building Room S068B, Stanford, CA 94305

<sup>3</sup>Orthopaedic Surgery, Stanford University, Stanford, California, USA

### Abstract

Conventional, static magnetic resonance imaging (MRI) is able to provide a vast amount of information regarding the anatomy and pathology of the musculoskeletal system. However, patients, especially those whose pain is position dependent or elucidated by movement, may benefit from more advanced imaging techniques that allow for the acquisition of functional information. This manuscript reviews a variety of advancements in magnetic resonance imaging techniques that are used to image the musculoskeletal system dynamically, while in motion or under load. The methodologies, advantages and drawbacks of Stress MRI, Cine PC MRI and Real-Time MRI are discussed as each has helped to advance the field by providing a scientific basis for understanding normal and pathological musculoskeletal anatomy and function. Advancements in dynamic MR imaging will certainly lead to improvements in the understanding, prevention, diagnosis and treatment of musculoskeletal disorders. It is difficult to anticipate that dynamic MRI will replace conventional MRI, however, dynamic MRI may provide additional valuable information to findings of conventional MRI.

### Keywords

Magnetic resonance imaging; dynamic imaging; kinematics

## INTRODUCTION

Accurate, *in vivo* measurements of joint loading and motion are necessary to the understanding of joint mechanics and the effective diagnosis and treatment of musculoskeletal pathology. Originally motivated by the fact that many pathologies arise

---

© 2011 OsteoArthritis Society International. Published by Elsevier Ltd. All rights reserved.

Garry E. Gold, 1201 Welch Road P271, Stanford, CA 94305, (O): 650-736-7518, (F): 650-725-7296, gold@stanford.edu.

**AUTHOR CONTRIBUTIONS:** Dr. Garry E. Gold and Lauren M. Shapiro have both made substantial contributions to all of the three sections listed: 1) the conception and design of the study, or acquisition of data, or analysis and interpretation of data, 2) drafting the article or revising it critically for important intellectual content and 3) final approval of the version to be submitted. Both authors contributed to the article's conception and design, analysis and interpretation of the data, drafting of the article, critical revision of the article for important intellectual content, final approval of the article, provision of study materials or patients, statistical expertise, obtaining of funding, administrative, technical or logistical support, and the collection and assembly of data. Both Dr. Gold (gold@stanford.edu) and Lauren M. Shapiro (laurenms09@gmail.com) take responsibility for the integrity of the work as a whole, from inception to finished article.

**CONFLICT OF INTEREST:** G.E.G. received research support from General Electric.

**Publisher's Disclaimer:** This is a PDF file of an unedited manuscript that has been accepted for publication. As a service to our customers we are providing this early version of the manuscript. The manuscript will undergo copyediting, typesetting, and review of the resulting proof before it is published in its final citable form. Please note that during the production process errors may be discovered which could affect the content, and all legal disclaimers that apply to the journal pertain.

from and affect joints during loading or movement, much work has been done to understand the roles of abnormal joint mechanics in the progression of musculoskeletal disorders. For example, the altered joint mechanics associated with both anterior cruciate ligament (ACL) deficient and ACL reconstructed knees are associated with and may contribute to the development and progression of osteoarthritis<sup>1-3</sup>. Additionally, abnormal patellofemoral joint kinematics is often cited as a risk factor for the development and progression of patellofemoral pain<sup>4-5</sup>. Techniques allowing the understanding of healthy joint mechanics as well as abnormal joint mechanics will respectively enable practitioners to establish normative values and diagnose, evaluate and treat musculoskeletal disorders.

Several methods for measuring joint mechanics exist and have been successful in enabling practitioners to better understand joint alignments, loading and kinematics. In the past, data of joint loading and motion have typically been collected from cadaveric studies and external measurements of limb movements obtained with motion capture methods<sup>6-9</sup>. Although helpful, these measurement techniques often fail to accurately replicate the complexities of a joint since cadaveric studies do not imitate *in vivo* conditions and motion capture techniques are based upon surface anatomy through the use of skin-based marker systems<sup>9</sup>. More precise methods of obtaining *in vivo* joint mechanics have been developed. One of these techniques involves attaching optical markers intracortically to obtain measurements of bone motion during functional tasks. This method, although providing much insight to *in vivo* bone kinetics and having accuracies of 0.5 mm, has its disadvantages<sup>10</sup>. The process of attaching the markers to the bones of interest is both invasive and difficult to perform; additionally, this technique provides little information with regard to the mechanics of the surrounding soft tissue. Other methods that still permit accurate measurements of bone mechanics include fluoroscopy and biplane radiography. Both enable direct visualization of bone mechanics during dynamic tasks, however they are limited since they are projective imaging modalities and three-dimensional (3D) registration must be performed to provide a clinical perspective and accurate 3D measurements<sup>11</sup>. These methods may utilize a marker-based registration technique<sup>12-14</sup> or an intensity-based registration technique<sup>12,15-18</sup>. The former, although having reported accuracies of 0.06 mm<sup>11, 13</sup> - 1.0 mm<sup>11, 12</sup> plane and 0.06 mm<sup>11, 13</sup> - 2.1 mm<sup>11, 12</sup> out of plane, requires the implantation of fiducial bone markers, exposes the subject to ionizing radiation and provides little information about the surrounding soft tissues. Intensity-based registration, which is often derived from a 3D model obtained with images from a computed tomography (CT) scanner, suffers in that it also exposes the subject to ionizing radiation and provides little information about the surrounding soft tissue. This registration method has reported accuracies of 0.42 mm<sup>11, 16</sup> - 1.74 mm<sup>11, 12</sup> in plane and 1.58 mm<sup>11, 12</sup> - 5.6 mm<sup>11, 16</sup> out of plane.

Due to its high resolution, noninvasive nature and multiplanar imaging capabilities, magnetic resonance imaging (MRI) has emerged as a promising method for imaging the musculoskeletal system<sup>19</sup>. It is an especially useful tool with which to evaluate soft tissue structures around joints *in vivo* as it permits one to manipulate contrast. Conventional MR imaging is typically carried out under non-weight bearing, non-dynamic conditions, however many recent advances in the field enable a more physiologic evaluation of the joints.

## STRESS MRI

One of the recent advances in the field of MR imaging is a technique called stress MRI. A stress MRI takes place in atypical positions or when a joint is under a load. This technique emerged in recognition of the fact that pain typically arises and affects joints during loaded positions or in positions dependent upon stress conditions. Several studies have confirmed

that static, unloaded positions are not representative of physiological or loaded positions and that in a clinical setting, evaluating a patient in the non-weight-bearing position alone may result in misdiagnoses<sup>20-24</sup>. It is important to recognize and appreciate the complex interactions of the various forces at play on the joints whether they are active muscular forces or dynamic physical forces, such as gravitational, contact or inertial<sup>25, 26</sup>.

Two primary means of obtaining a stress MRI are accomplished through the use of an upright open-bore MRI scanner and a supine closed-bore scanner that may utilize a weight bearing apparatus. Most commonly used for the knee, the upright open-bore scanner that may utilize a custom back support, enables the MR image to be acquired under physiologic, loaded and even flexed conditions<sup>27</sup>. The use of the back support system is limited, yet expanding. Figures 1a and 1b are examples of the double doughnut configuration<sup>28</sup>. The drawback of this imaging technique lies in the lower field strength of open-bore scanners resulting in a lower resolution due to a decreased signal-to-noise ratio<sup>28</sup>. The closed-bore option can be used to image weight-bearing, atypical positioning, functional positions or some combination of variants. Although a harness and footplate may be used to simulate weight-bearing in a closed-bore MR system, it may not allow for the appreciation of all aspects of upright loading, as the closed-bore system tends to limit the patient's range of flexion<sup>28</sup> Figure 1c. There are, however, new wide-bore (70cm) 3.0T MR systems that provide high field supine imaging that allow for more stress and motion possibilities. As with any weight bearing system, a relevant limitation is that of muscle fatigue. Additionally, consideration must be taken to select a high-quality RF coil that does not limit the motion being studied. Of important note is the lack of these scanners in clinical use due primarily to the considerations taken into account when purchasing a scanner. In a clinical setting, the ability to conduct high resolution supine MR imaging, especially of the brain and spine, is critically important. For this reason, the use of horizontal closed-bore scanners with harnesses and footplates is a common supine alternative to upright open-bore MR imaging. Table 1 and Table 2 highlight the advantages and drawbacks of using an open configuration and a supine closed-bore MR imaging system, respectively.

The applications of stress MR imaging often outweigh the systems' inherent limitations. As previously mentioned, pain is often elicited in only certain positions or under loaded conditions, making stress MR imaging often more beneficial than conventional MR imaging under particular conditions. Studies have shown that compared to a routine MR image, an axial loaded MR image of the spine can provide additional valuable information and can influence physicians' treatment decisions<sup>29, 30</sup>.

Stress MR imaging techniques, which have been demonstrated to have strong accuracy and subject-repeatability measures, have also led to an increased amount of knowledge regarding the physiology and biomechanics of important tissues within the joints<sup>31,32</sup> Table 3. Some of this research has focused on the patellofemoral joint, as patellofemoral pain syndrome (PFPS) is a frequent cause of knee pain. Gold et al. demonstrated that with an open-bore scanner and a custom back support, it is feasible to image patellar cartilage accurately during physiologic loading<sup>28</sup>. The increase in the cartilage contact area in the patellofemoral joint under a load that the group observed displays the potential of stress MR imaging in the understanding, evaluation and treatment of PFPS and the patellofemoral joint as a whole<sup>28</sup> Figure 2. Kinematic joint changes, thought to be an important factor in the onset and progression of osteoarthritis (OA), have been evaluated in healthy, ACL-deficient and ACL-reconstructed knees with the stress MRI technique<sup>33, 34</sup>. Imaging at various degrees of flexion and extension has allowed clinicians to obtain more physiologic measurements of contact area centroid locations in healthy, pathologic and reconstructed knees leading to a better kinematic understanding of the joints<sup>35</sup>. As OA has grown to affect over 27 million adults in the United States, the understanding of this disease and its risk factors becomes

increasingly more important<sup>36</sup>. Menisci of the knee are congruent to the tibial and femoral condyles and among many things, function to absorb shock and transmit the load of the weight of the body. In order to appropriately accommodate the body's position and facilitate load distribution, the menisci are adaptable and shift with respect to the articular surfaces to increase surface area<sup>37-39</sup>. Studies have demonstrated that in knee flexion, both the medial and the lateral menisci posteriorly translate on the tibial plateau and that upon conditions of loading, the menisci shift, most significantly in the anterior horn of the lateral meniscus, to accommodate the stress<sup>40, 41</sup>. Understanding of these meniscal dynamics may have clinical relevance to diagnosis, prevention and treatment of meniscal injury.

Since the shoulder has the widest range of motion of any joint in the body, the space and flexibility provided by open MR units suit imaging of the shoulder joint well<sup>42</sup>. The open configuration of the system allows a technologist or radiologist to perform clinical stress testing and interventional procedures to carry out an all-in-one MR arthrography and evaluate the joint for the presence and direction of glenohumeral instability<sup>43-46</sup>. These evaluations stand to decrease the number of extra personnel and transportation needed to move a patient between rooms and can provide valuable information to the surgeon designing a treatment or surgical plan<sup>43, 47</sup>.

## CINE PC MRI

Cine phase contrast (cine-PC) MR imaging, originally developed to study flow and motion in the cardiovascular system, is a noninvasive, *in vivo* kinematic technique capable of measuring 3D velocities of tissue within an imaging plane during tasks involving movement<sup>48, 49</sup>. Cine-PC MR imaging was developed through the combination of two separate MR imaging techniques. The first of which, cine MRI, produces a series of quasi-static anatomic images at various stages of the motion cycle during a single acquisition. The object and motion being imaged must be repeatable and gated to the MR data acquisition. Cine MR imaging collects data continuously over several cycles and retrospectively sorts data with a synchronization trigger in order to compensate for periodic motion<sup>48</sup>. The second technique, phase contrast MR imaging, quantifies local velocity and creates a velocity map by using velocity-dependent pulse sequences to extract the velocity from the phase of signal<sup>48</sup>. By combining these two techniques, cine-PC MR imaging provides an anatomic image and three orthogonal velocity images ( $v_x$ ,  $v_y$ ,  $v_z$ ) for each frame<sup>48</sup>. Cine-PC MR imaging has been shown to be a promising method with which to study knee joint kinematics<sup>48, 50, 51</sup>. In recent studies conducted by Behnam et al., cine-PC MRI has been demonstrated to have strong accuracy and subject-repeatability in the assessment of *in vivo* musculoskeletal motion tracking at 3.0T<sup>31</sup> Table 3.

The primary drawback of cine-PC MR imaging is that it requires multiple repetitions of the same motion cycle, which subsequently presents more challenges. If the motion cycles are not repeated accurately, the image quality can degrade significantly. Only small loads upon the body can be tested as multiple motion cycles may lead to subject fatigue. Additionally, subjects with conditions that do not allow them to perform the repeated action being studied may 1) require the investigator to passively move the subject's limb or 2) may not be able to be studied with cine-PC MR imaging. Finally, as these techniques were developed to image the flow and motion in the cardiovascular system, imaging musculoskeletal velocities, which are significantly slower, presents a challenge. To use cine-PC MR imaging to measure slower velocities, a larger encoding gradient is necessary<sup>49, 52</sup>.

Despite these drawbacks, cine-PC MR imaging has been used to gain vast amounts of understanding in reference to musculoskeletal structure and function. Cine-PC MR imaging has been used by Asakawa et al. to further understand muscle mechanics following tendon

transfer surgery<sup>53</sup>, by Pappas et al. to challenge the conventional thinking that muscle fascicles shorten uniformly<sup>54</sup> and by Finni et al.<sup>55, 56</sup> to investigate the complex deformations of the isometrically contracting soleus muscle. Recently, cine-PC imaging has been used by Bradford et al. with PC-VIPR to measure tibio-femoral kinematics and to visualize cartilage contact during movement in the hopes of teasing out the etiology of early onset OA following ACL reconstruction<sup>57</sup> Figure 3. Cine-PC imaging has also been used by Hodgson et al. to track and study the strain along the aponeurosis-tendon length<sup>58</sup>. In this manner, a trajectory is calculated for every pixel and strain distribution can be seen at all times throughout the contraction cycle. In studying particular muscles with the cine-PC MR imaging technique, a better understanding of how specific muscles produce force and displacement can be acquired<sup>58</sup>.

Since muscle deformations are often highly complex and 3D, they can be better understood with MR tagging and MR imaging with displacement encoding with simulated echoes (DENSE) techniques, which are better approaches to extracting fine resolution displacements and strain fields than cine-PC MR imaging<sup>9</sup>. Spin tagging is accomplished by inverting spatially separated thin bands of protons and allowing motion visualizing as distorted tagged lines in subsequent temporal phases<sup>9, 59-61</sup>. Unfortunately, spin tagging lacks information between tags and experiences tag line fading<sup>9</sup>. It has, however, been used to understand myocardial wall and skeletal muscle motion as it enables a deeper appreciation of three-dimensional tissue motion<sup>56, 62</sup>. DENSE MR imaging encodes tissue displacement into the phase of the stimulated echo by encoding motion over long time intervals<sup>31, 63</sup>. To date, several researchers have successfully utilized DENSE to evaluate strain within myocardial tissue<sup>31, 63, 64</sup>. By using DENSE MR imaging, Zhong et al. demonstrated *in vivo* skeletal muscle mechanics to a level of precision that was not previously possible. By illustrating that two-dimensional strains during low-load elbow flexion were nonuniform throughout the biceps brachii muscle, they exemplified the complex multi-dimensional deformation of skeletal muscle that occurs during contraction<sup>65</sup> Figure 4.

## REAL TIME MRI

Real-time MRI, in addition to also originating as a technique with which to image cardiovascular motion and flow, holds great promise in the evaluation of joints during volitional tasks<sup>11, 66</sup>. Real-time MR imaging, although primarily conducted in 2D in the musculoskeletal system, is advantageous as it acquires a time series of single image slices in only one motion cycle and the velocities that are measured are not averaged over multiple cycles of motion. In contrast to cine-PC MR imaging, by only requiring one motion cycle, real-time MR imaging makes subject fatigue less of a concern and permits subjects with conditions preventing them from repeating certain movements to be evaluated. Fatigue is also minimized as image plane data can be acquired quickly with real-time MRI and can be reconstructed with image display rates of 24 frames/sec<sup>11, 67</sup>. Additionally, the imaging plane can be continuously defined and updated in real-time to continue tracking an object if motion out of the imaging plane occurs<sup>67</sup>.

It should be noted that the accuracy associated with real-time MRI is highly dependent upon the type of scanner used. The signal-to-noise ratio, the acquisition frame rate and the image resolution all affect accuracy and are, themselves, dependent upon the slew rate and magnitude of the gradients, the homogeneity of the main magnetic field and the field strength of the scanner<sup>11</sup>. Although cine-PC MR imaging has slightly better accuracy and repeatability measurements, real-time MRI may be more desirable for those subjects who fatigue easily or those who are unable to repetitively perform the movement being imaged<sup>11, 21, 68</sup> Table 3.

To accompany and enhance the development of kinematic imaging with real-time MRI many hardware and software advancements have been made. Flexible knee coils have been developed, tested and shown, in a very few number of subjects, to have similar results to static data while reporting high SNR values and homogenous coverage<sup>69, 70</sup>. A high-resolution steady-state free precession (SSFP) pulse sequence was applied to track bone motion with real-time MR imaging. Upon testing and with the use of shape-matching algorithms, 3D *in vivo* joint kinematics were accurately established with millimeter resolution<sup>71</sup>.

Draper et al., recently used real-time MR imaging to demonstrate the differences in weight-bearing response and measured patellofemoral kinematics between subjects with patellofemoral maltracking and those without<sup>21</sup> Figure 5. The measurement of moment arms is another valuable application to which real-time MR imaging has proved useful. A moment arm, the perpendicular distance from the joint center to a particular muscle's line of action, defines the function of a muscle around a particular joint and can verify the accuracy of representations of muscle paths<sup>72</sup>. Like many of the previously discussed applications, the measurement of moment arms has traditionally been estimated with cadaveric<sup>73</sup>, ultrasound<sup>74</sup>, CT<sup>75</sup> and static MRI<sup>76-78</sup> studies. Blemker and McVeigh have demonstrated the feasibility of the measurement of moment arms in the knee throughout its full range of motion with the real-time MR imaging technique in a wide-bore scanner<sup>9, 79</sup> Figure 6. The ability to characterize moment arms under more physiologic conditions with kinematic imaging techniques is a powerful technology made even more valuable when performed in combination with other MR-based applications as comparisons can be made between the image data and the model<sup>9</sup>.

A slight variation of real-time MR imaging is real-time PC MR imaging which can be applied to measure *in vivo* skeletal muscle velocity during dynamic motion<sup>52</sup>. As this method was, again, initially developed to image cardiac flow, modifications were made in order to image slower musculoskeletal motion. Asakawa et al. demonstrated the ability to acquire accurate measurements of encoded velocities in both the biceps brachii and triceps brachii using real-time PC MR imaging<sup>52</sup>. Similar to the previous applications of real-time MR imaging, this technique is valuable, as it requires only one motion cycle while providing a means of understanding musculoskeletal structure and function.

## CONCLUSION

In the above review, several MR imaging methods that enable a better understanding of functional aspects of the musculoskeletal system are described. The data acquired from these techniques has helped to advance the field by developing more realistic models of the musculoskeletal framework and helping to answer important biomechanical questions. While the novelty of these functional imaging techniques holds potential in advancing the field, the primary application of these imaging techniques is still within the research realm where the focus is currently centered around the optimization of such techniques. The developments presented by the described methods can be combined with other image-based musculoskeletal modeling techniques and have already begun to provide clinically useful insights and revolutionize the study of musculoskeletal anatomy, pathology and function.

## Acknowledgments

Funding acknowledgments include NIH EB002524, NIH EB005790, General Electric Healthcare and SCBT/MR. Funding from these sources allowed for the conception and design of the study as well as the acquisition, analysis and interpretation of the data. Funding also allowed for the drafting and revision of the article.

## References

1. Barrance PJ, Williams GN, Snyder-Mackler L, Buchanan TS. Altered knee kinematics in ACL-deficient non-copers: a comparison using dynamic MRI. *J Orthop Res.* 2006; 24:132–40. [PubMed: 16435346]
2. Butler RJ, Minick KI, Ferber R, Underwood F. Gait mechanics after ACL reconstruction: implications for the early onset of knee osteoarthritis. *Br J Sports Med.* 2009; 43:366–70. [PubMed: 19042923]
3. Streich NA, Zimmermann D, Bode G, Schmitt H. Reconstructive versus non-reconstructive treatment of anterior cruciate ligament insufficiency. A retrospective matched-pair long-term follow up. *Int Orthop.* 2010; 35:607–13. [PubMed: 21127860]
4. Fulkerson JP. Diagnosis and treatment of patients with patellofemoral pain. *Am J Sports Med.* 2002; 30:447–56. [PubMed: 12016090]
5. LaBella C. Patellofemoral pain syndrome: evaluation and treatment. *Prim Care.* 2004; 31:977–1003. [PubMed: 15544830]
6. Mizuno Y, Kumagai M, Mattessich SM, Elias JJ, Ramrattan N, Cosgarea AJ, et al. Q-angle influences tibiofemoral and patellofemoral kinematics. *J Orthop Res.* 2001; 19:834–40. [PubMed: 11562129]
7. Amis AA, Senavongse W, Bull AM. Patellofemoral kinematics during knee flexion-extension: an in vitro study. *J Orthop Res.* 2006; 24:2201–11. [PubMed: 17004269]
8. Andriacchi TP, Alexander EJ, Toney MK, Dyrby C, Sum J. A point cluster method for *in vivo* motion analysis: applied to a study of knee kinematics. *J Biomech Eng.* 1998; 120:743–49. [PubMed: 10412458]
9. Blemker SS, Asakawa DS, Gold GE, Delp SL. Image-based musculoskeletal modeling: applications, advances, and future opportunities. *J Magn Reson Imaging.* 2007; 25:441–51. [PubMed: 17260405]
10. Ishii Y, Terajima K, Terashima S, Koga Y. Three-dimensional kinematics of the human knee with intracortical pin fixation. *Clin Orthop Relat Res.* 1997; 343:144–50. [PubMed: 9345219]
11. Draper CE, Santos JM, Kourtis LC, Besier TF, Fredericson M, Beaupre GS, et al. Feasibility of using real-time MRI to measure joint kinematics in 1.5T and open-bore 0.5T systems. *J Magn Reson Imaging.* 2008; 28:158–66. [PubMed: 18581329]
12. Tang TS, MacIntyre NJ, Gill HS, Fellows RA, Hill NA, Wilson DR, et al. Accurate assessment of patellar tracking using fiducial and intensity-based fluoroscopic techniques. *Med Image Anal.* 2004; 8:343–51. [PubMed: 15450227]
13. Tashman S, Anderst W. In-vivo measurement of dynamic joint motion using high speed biplane radiography and CT: application to canine ACL deficiency. *J Biomech Eng.* 2003; 125:238–45. [PubMed: 12751286]
14. Tashman S, Collon D, Anderson K, Kolowich P, Anderst W. Abnormal rotational knee motion during running after anterior cruciate ligament reconstruction. *Am J Sports Med.* 2004; 32:975–83. [PubMed: 15150046]
15. Bey MJ, Zael R, Brock SK, Tashman S. Validation of a new model-based tracking technique for measuring three-dimensional, *in vivo* glenohumeral joint kinematics. *J Biomech Eng.* 2006; 128:604–9. [PubMed: 16813452]
16. Fregly BJ, Rahman HA, Banks SA. Theoretical accuracy of model-based shape matching for measuring natural knee kinematics with single-plane fluoroscopy. *J Biomech Eng.* 2005; 127:692–9. [PubMed: 16121540]
17. Komistek RD, Dennis DA, Mahfouz M. *In vivo* fluoroscopic analysis of the normal human knee. *Clin Orthop Relat Res.* 2003; 410:69–81. [PubMed: 12771818]
18. You BM, Siy P, Anderst W, Tashman S. *In vivo* measurement of 3-D skeletal kinematics from sequences of biplane radiographs: application to knee kinematics. *IEEE Trans Med Imaging.* 2001; 20:514–25. [PubMed: 11437111]
19. Resnick, D.; Kang, H. *Internal derangements of joints.* New York, NY: Saunders; 1997.

20. Taschman S, Collon D, Anderson K, Kolowich P, Anderst W. Abnormal rotational knee motion during running after anterior cruciate ligament reconstruction. *Am J Sports Med.* 2004; 32:975–83. [PubMed: 15150046]
21. Draper CE, Besier TF, Fredericson M, Santos JM, Beaupre GS, Delp SL, et al. Differences in patellofemoral kinematics between weight-bearing and non-weight-bearing conditions in patients with patellofemoral pain. *J Orthop Res.* 2010; 29:312–7. [PubMed: 20949442]
22. Shellock FG, Mink JH, Deutsch AL, Foo TK, Sullenberger P. Patellofemoral joint: identification of abnormalities with active-movement, “unloaded” versus “loaded” kinematic MR imaging techniques. *Radiology.* 1993; 188:575–8. [PubMed: 8327718]
23. Powers CM, Ward SR, Fredericson M, Guillet M, Shellock FG. Patellofemoral kinematics during weight-bearing and non-weight-bearing knee extension in persons with lateral subluxation of the patella: a preliminary study. *J Orthop Sports Phys Ther.* 2003; 33:677–85. [PubMed: 14669963]
24. McWalter EJ, Hunter DJ, Wilson DR. The effect of load magnitude on three-dimensional patellar kinematics *in vivo*. *J Biomech.* 2010; 43:1890–7. [PubMed: 20413124]
25. Markolf KL, Bargar WL, Shoemaker SC, Amstutz HC. The role of joint load in knee stability. *J Bone Joint Surg Am.* 1981; 63:570–85. [PubMed: 7217123]
26. Schipplein OD, Andriacchi TP. Interaction between active and passive knee stabilizers during level walking. *J Orthop Res.* 1991; 9:113–9. [PubMed: 1984041]
27. Besier T, Pal S, Draper C, Fredericson M, Gold G, Delp S, et al. Musculoskeletal modelling and imaging to understand patellofemoral pain. IUTAM. 2010 abstract.
28. Gold GE, Besier TF, Draper CE, Asakawa DS, Delp SL, Beauré G. Weight-bearing MRI of patellofemoral joint cartilage contact area. *J Magn Reson Imaging.* 2004; 20:526–30. [PubMed: 15332263]
29. Hiwatashi A, Danielson B, Moritani T, Bakos RS, Rodenhause TG, Pilcher WH, et al. Axial loading during MR imaging can influence treatment decision for symptomatic spinal stenosis. *AJNR Am J Neuroradiol.* 2004; 25:170–4. [PubMed: 14970014]
30. Willén J, Danielson B. The diagnostic effect from axial loading of the lumbar spine during computed tomography and magnetic resonance imaging in patients with degenerative disorders. *Spine.* 2001; 26:2607–14. [PubMed: 11725243]
31. Behnam AJ, Herzka DA, Sheedan FT. Assessing the accuracy and precision of musculoskeletal motion tracking using cine-PC MRI on a 3.0T platform. *J Biomech.* 2011; 44:193–7. [PubMed: 20863502]
32. Fellows RA, Hill NA, Macintyre NJ, Harrison MM, Ellis RE, Wilson DR. Repeatability of a novel technique for *in vivo* measurement of three-dimensional patellar tracking using magnetic resonance imaging. *J Magn Reson Imaging.* 2005; 22:145–53. [PubMed: 15971173]
33. Carpenter RD, Majumdar S, Ma CB. Magnetic resonance imaging of 3-dimensional *in vivo* tibiofemoral kinematics in anterior cruciate ligament-reconstructed knees. *Arthroscopy.* 2009; 25:760–6. [PubMed: 19560640]
34. Shin CS, Carpenter RD, Majumdar S, Ma CB. Three-dimensional *in vivo* patellofemoral kinematics and contact area of anterior cruciate ligament-deficient and –reconstructed subjects using magnetic resonance imaging. *Arthroscopy.* 2009; 25:1214–23. [PubMed: 19896042]
35. Shefelbine SJ, Ma CB, Lee KY, Schrupf MA, Patel P, Safran MR, et al. MRI analysis of *in vivo* meniscal and tibiofemoral kinematics in ACL-deficient and normal knees. *J Orthop Res.* 2006; 24:1208–17. [PubMed: 16652339]
36. Lawrence RC, Felson DT, Helmick CG, Arnold LM, Choi H, Deyo RA, et al. Estimates of the prevalence of arthritis and other rheumatic conditions in the United States. Part II. *Arthritis Rheum.* 2008; 58:26–35. [PubMed: 18163497]
37. Thompson WO, Thaete FL, Fu FH, Dye SF. Tibial meniscal dynamics using three-dimensional reconstruction of magnetic resonance images. *Am J Sports Med.* 1991; 19:210–215. discussion 215–216. [PubMed: 1867329]
38. Bylski-Austrow DI, Ciarelli MJ, Kayner DC, Matthews LS, Goldstein SA. Displacements of the menisci under joint load: an *in vitro* study in human knees. *J Biomech.* 1994; 27:421–31. [PubMed: 8188723]



39. Kessler MA, Glaser C, Tittel S, Reiser M, Imhoff AB. Volume changes in the menisci and articular cartilage of runners: an *in vivo* investigation based on 3-D magnetic resonance imaging. *Am J Sports Med.* 2006; 34:832–6. [PubMed: 16436539]
40. Vedi V, Williams A, Tennant SJ, Spouse E, Hunt DM, Gedroyc WM. Meniscal movement. An *in vivo* study using dynamic MRI. *J Bone Joint Surg Br.* 1999; 81:37–41. [PubMed: 10067999]
41. Yao J, Lancianese SL, Hovinga KR, Lee J, Lerner AL. Magnetic resonance image analysis of meniscal translation and tibio-menisco-femoral contact in deep knee flexion. *Ortop Res.* 2008; 26:673–84.
42. Rockwood, C.; Matsen, FA. Clinical evaluation of shoulder problems. The Shoulder Saunders; Philadelphia: 1998. p. 149-77.
43. Vandevenne JE, Vanhoenacker F, Beaulieu CF, Bergman AG, Butts Pauly K, Dillingham MF, et al. All-in-one magnetic resonance arthrography of the shoulder in a vertically open magnetic resonance unit. *Acta Radiol.* 2008; 49:918–27. [PubMed: 18651257]
44. Genant J, Vandevenne JE, Bergman AG, Beaulieu CF, Kee ST, Norbash AM, et al. Interventional musculoskeletal procedures performed by using MR imaging guidance with a vertically open MR unit: assessment of techniques and applicability. *Radiology.* 2002; 223:127–36. [PubMed: 11930057]
45. Hodge DK, Beaulieu CF, Thabit GH 3rd, Gold GE, Bergman AG, Butts RK, et al. Dynamic MR imaging and stress testing in glenohumeral instability: comparison with normal shoulders and clinical/surgical findings. *J Magn Reson Imag.* 2001; 13:748–56.
46. Pappas GP, Blemker SS, Beaulieu CF, McAdams TR, Whalen ST, Gold GE. *In vivo* anatomy of the Neer and Hawkins sign positions for shoulder impingement. *J Shoulder Elbow Surg.* 2006; 15:40–9. [PubMed: 16414467]
47. Andreisek G, Duc SR, Froehlich JM, Hodler J, Weishaupt D. MR arthrography of the shoulder, hip, and wrist: evaluation of contrast dynamics and image quality with increasing injection-to-imaging time. *AJR Am J Roentgenol.* 2007; 188:1081–8. [PubMed: 17377051]
48. Sheehan FT, Zajac FE, Drace JE. Using cine phase contrast magnetic resonance imaging to non-invasively study *in vivo* knee dynamics. *J Biomech.* 1998; 31:21–6. [PubMed: 9596534]
49. Pelc NJ, Herfkens RJ, Shimakawa A, Enzmann DR. Phase contrast cine magnetic resonance imaging. *Magn Reson Q.* 1991; 7:229–54. [PubMed: 1790111]
50. Sheehan FT, Drace JE. Quantitative MR measures of three-dimensional patellar kinematics as a research and diagnostic tool. *Med Sci Sports Exerc.* 1999; 31:1399–405. [PubMed: 10527311]
51. Sheehan FT, Zajac FE, Drace JE. *In vivo* tracking of the human patella using cine phase contrast magnetic resonance imaging. *J Biomech Eng.* 1999; 121:650–6. [PubMed: 10633267]
52. Asakawa DS, Nayak KS, Blemker SS, Delp SL, Pauly JM, Nishimura DG, et al. Real-time imaging of skeletal muscle velocity. *J Magn Reson Imaging.* 2003; 18:734–9. [PubMed: 14635159]
53. Asakawa DS, Blemker SS, Gold GE, Delp SL. *In vivo* motion of the rectus femoris muscle after tendon transfer surgery. *J Biomech.* 2002; 35:1029–37. [PubMed: 12126662]
54. Pappas GP, Asakawa DS, Delp SL, Zajac FE, Drace JE. Nonuniform shortening in the biceps brachii during elbow flexion. *J Appl Physiol.* 2002; 92:2381–9. [PubMed: 12015351]
55. Finni T, Hodgson JA, Lai AM, Edgerton VR, Sinha S. Mapping of movement in the isometrically contracting human soleus muscle reveals details of its structural and functional complexity. *J Appl Physiol.* 2003; 95:2128–33. [PubMed: 12857769]
56. Sinha S, Hodgson JA, Finni T, Lai AM, Grinstead J, Edgerton VR. Muscle kinematics during isometric contraction: development of phase contrast and spin tag techniques to study healthy and atrophied muscles. *J Magn Reson Imaging.* 2004; 20:1008–19. [PubMed: 15558560]
57. Bradford R, Johnson K, Wieben O, Thelen D. Dynamic imaging of 3d knee kinematics using PC-VIPR. *ISMRM.* 2011 [abstract] Abstract #3178.
58. Hodgson JA, Finni T, Lai AM, Edgerton R, Sinha S. Influence of structure on the tissue dynamics of the human soleus muscle observed in MRI studies during isometric contraction. *J Morphol.* 2006; 267:584–601. [PubMed: 16453292]

59. Finni T, Hodgson JA, Lai AM, Edgerton VR, Sinha S. Non-uniform strain of human soleus aponeurosis-tendon complex during submaximal voluntary contractions *in vivo*. *J Appl Physiol*. 2003; 95:829–37. [PubMed: 12716873]
60. Shellock FG, Fleckenstein JL. Muscle physiology and pathophysiology: magnetic resonance imaging evaluation. *Semin Musculoskelet Radiol*. 2000; 4:459–79. [PubMed: 11371329]
61. Zerhouni EA, Parish DM, Rogers WJ, Yang A, Shapiro EP. Human heart: tagging with MR imaging—a method for noninvasive assessment of myocardial motion. *Radiology*. 1988; 169:59–63. [PubMed: 3420283]
62. Declerck J, Denney TS, Oztürk C, O'Dell W, McVeigh ER. Left ventricular motion reconstruction from planar tagged MR images: a comparison. *Phys Med Biol*. 2000; 45:1611–32. [PubMed: 10870714]
63. Aletras AH, Ding S, Balaban RS, Wen H. DENSE: displacement encoding with stimulated echos in cardiac functional MRI. *J Magn Reson*. 1999; 137:247–52. [PubMed: 10053155]
64. Kim D, Gilson WD, Kramer CM, Epstein FH. Myocardial tissue tracking with two-dimensional cine displacement-encoded MR imaging: development and initial evaluation. *Radiology*. 2004; 230:862–71. [PubMed: 14739307]
65. Zhong X, Epstein FH, Spottiswoode BS, Helm PA, Blemker SS. Imaging two-dimensional displacements and strains in skeletal muscle during joint motion by cine DENSE MR. *J Biomech*. 2008; 41:532–40. [PubMed: 18177655]
66. Aletras AH, Balaban RS, Wen H. High-resolution strain analysis of the human heart with fast-DENSE. *J Magn Reson*. 1999; 140:41–57. [PubMed: 10479548]
67. Nayak KS, Cunningham CH, Santos JM, Pauly JM. Real-time cardiac MRI at 3 Tesla. *Magn Reson Med*. 2004; 51:655–60. [PubMed: 15065236]
68. Draper CE, Besier TF, Santos JM, Jennings F, Fredericson M, Gold GE, et al. Using real-time MRI to quantify altered joint kinematics in subjects with patellofemoral pain and to evaluate the effects of a patella brace or sleeve on joint motion. *J Orthop Res*. 2009; 27:571–7. [PubMed: 18985690]
69. d'Entremont AG, Nordemeyer-Massner J, Bos C, Wilson DR, Pruessmann K. A dynamic measurement method for knee biomechanics. ISMRM. 2010 [abstract] Abstract #3185.
70. Nordemeyer-Massner JA, De Zanche N, Pruessmann KP. Stretchable coil arrays enable knee imaging at varying flexion angles. ISMRM. 2008 [abstract] Abstract #2540.
71. Nayak KS, Hargreaves BA, Besier TF, Delp SL. High-resolution real-time MRI of knee kinematics. RSNA. 2003:A20–174. [abstract] Code.
72. Pandy MG. Moment arm of a muscle force. *Exerc Sport Sci Rev*. 1999; 27:79–118. [PubMed: 10791015]
73. Buford WL Jr, Ivey FM Jr, Malone JD, Patterson RM, Peare GL, Nguyen DK, et al. Muscle balance at the knee -- moment arms for the normal knee and the ACL-minus knee. *IEEE Trans Rehabil Eng*. 1997; 5:367–79. [PubMed: 9422462]
74. Ito M, Akima H, Fukunaga T. *In vivo* moment arm determination using B-mode ultrasonography. *J Biomech*. 2000; 33:215–8. [PubMed: 10653035]
75. Németh G, Ohlsén H. Moment arm lengths of trunk muscles to the lumbosacral joint obtained *in vivo* with computed tomography. *Spine*. 1986; 11:158–60. [PubMed: 3704803]
76. Rugg SG, Gregor RJ, Mandelbaum BR, Chiu L. *In vivo* moment arm calculations at the ankle using magnetic resonance imaging (MRI). *J Biomech*. 1990; 23:495–501. [PubMed: 2373722]
77. Jorgensen MJ, Marras WS, Granata KP, Wiand JW. MRI-derived moment-arms of the female and male spine loading muscles. *Clin Biomech*. 2001; 16:182–93.
78. Wilson DL, Zhu Q, Duerk JL, Mansour JM, Kilgore K, Crago PE. Estimation of tendon moment arms from three-dimensional magnetic resonance images. *Ann Biomed Eng*. 1999; 27:247–56. [PubMed: 10199701]
79. Blemker SS, McVeigh ER. Real-time measurements of knee muscle moment arms during dynamic knee flexion-extension motion. ISMRM. 2006 [abstract] Abstract #3619.

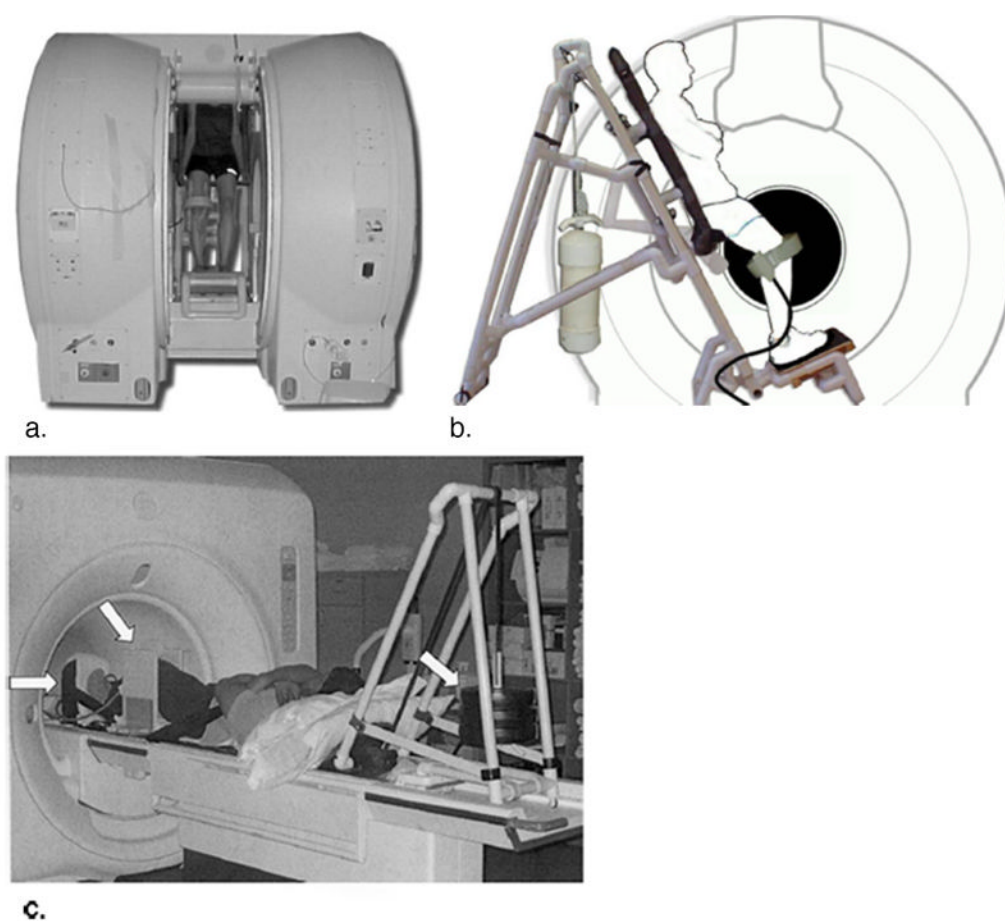


**Figure 1.** Subject and custom-built MR-compatible back support within the double doughnut configuration allowing for upright MR examination (a). Schematic of subject within the back support illustrating adjustable toggle to accommodate unloaded and loaded conditions (b). A seat rest can be made available upon pushing the toggle forward to allow the subject to sit down and support his or her own body weight. The back support slides up and down on rollers facilitating positions of knee flexion. A pulley and cleat mechanism is used to lock the back support into the desired position. A custom-made, weight-bearing apparatus that is compatible with closed MR scanners (c). The subject lays supine, with his or her knee of interest between the two plates of a knee holder (**middle arrow**) and his or her foot pushed on a footplate (**left arrow**). Weights, which hang behind the patient, (**right arrow**) are connected to the footplate by a loading strap. (Reproduced from Besier TF, Draper CE, Gold GE, Beaupre GS, Delp SL. Patellofemoral joint contact area increases with knee flexion and weight-bearing, *J Orthop Res* 2005;23:345-50, with permission of Wiley-Liss, Inc, a subsidiary of John Wiley & Sons, Inc. and Lee KY, Slavinsky JP, Ries MD, Blumenkrantz G, Majumdar S. Magnetic resonance imaging of *in vivo* kinematics after total knee arthroplasty, *J Magn Reson Imaging* 2005;21:172-8, with permission of Wiley-Liss, Inc, a subsidiary of John Wiley & Sons, Inc.)

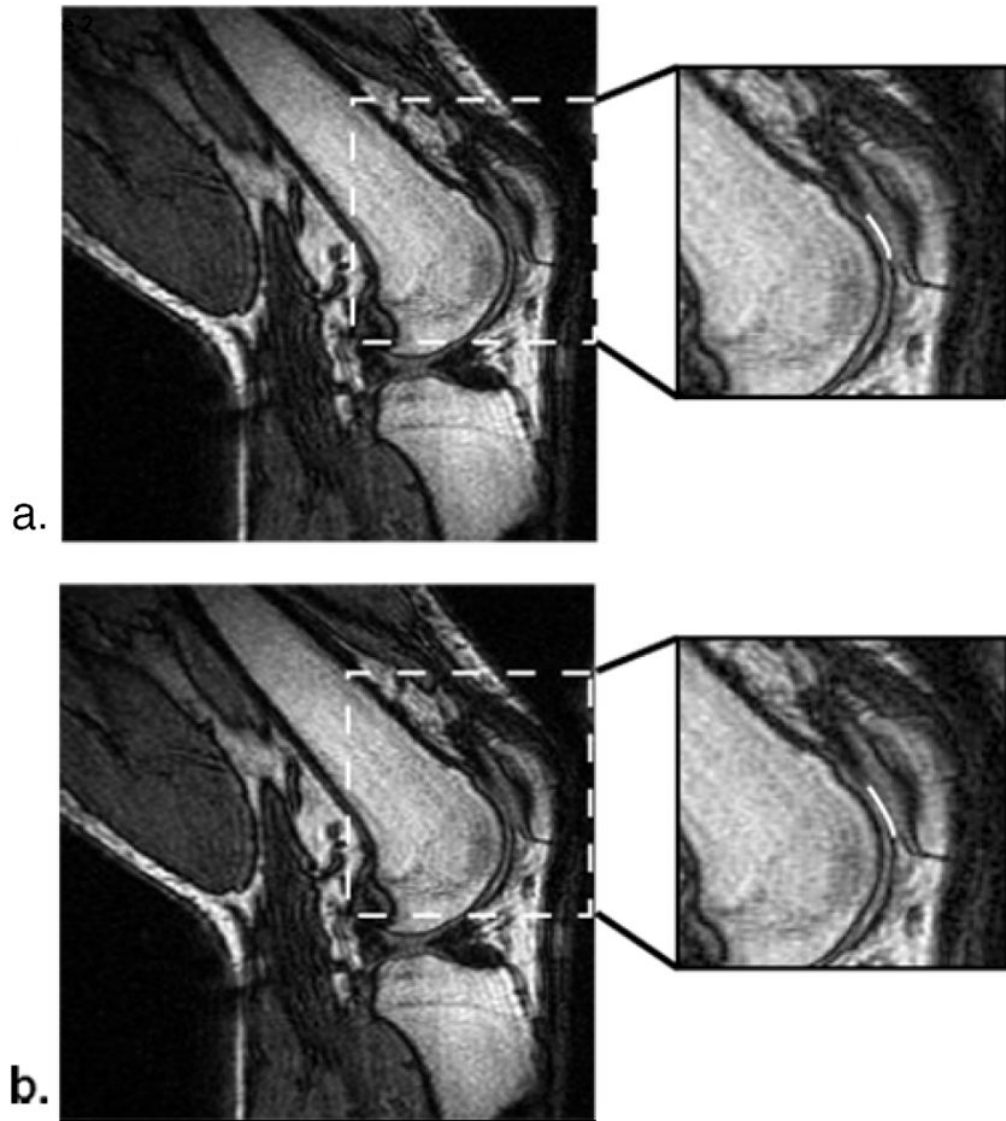


**Figure 2.** MR images (TR/TE: 33/9 msec, NEX: 1) of an unloaded (**a**) and loaded (**b**) knee of a healthy volunteer at 30° of flexion in 2:13 minutes with an approximate load of 0.45 times the subject's body weight supported by each leg. Contact regions (**white lines**) between the patella and femoral cartilage are displayed in the close up images. A slight increase in the contact region is apparent in the loaded image. Both images appear artifact free allowing for visualization of patellar cartilage. (Reproduced from Gold GE, Besier TF, Draper CE, Asakawa DS, Delp SL, Beaupre GS. Weight-bearing MRI of patellofemoral joint cartilage contact area, *J Magn Reson Imaging* 2004;20:526-30, with permission of Wiley-Liss, Inc, a subsidiary of John Wiley & Sons, Inc.)

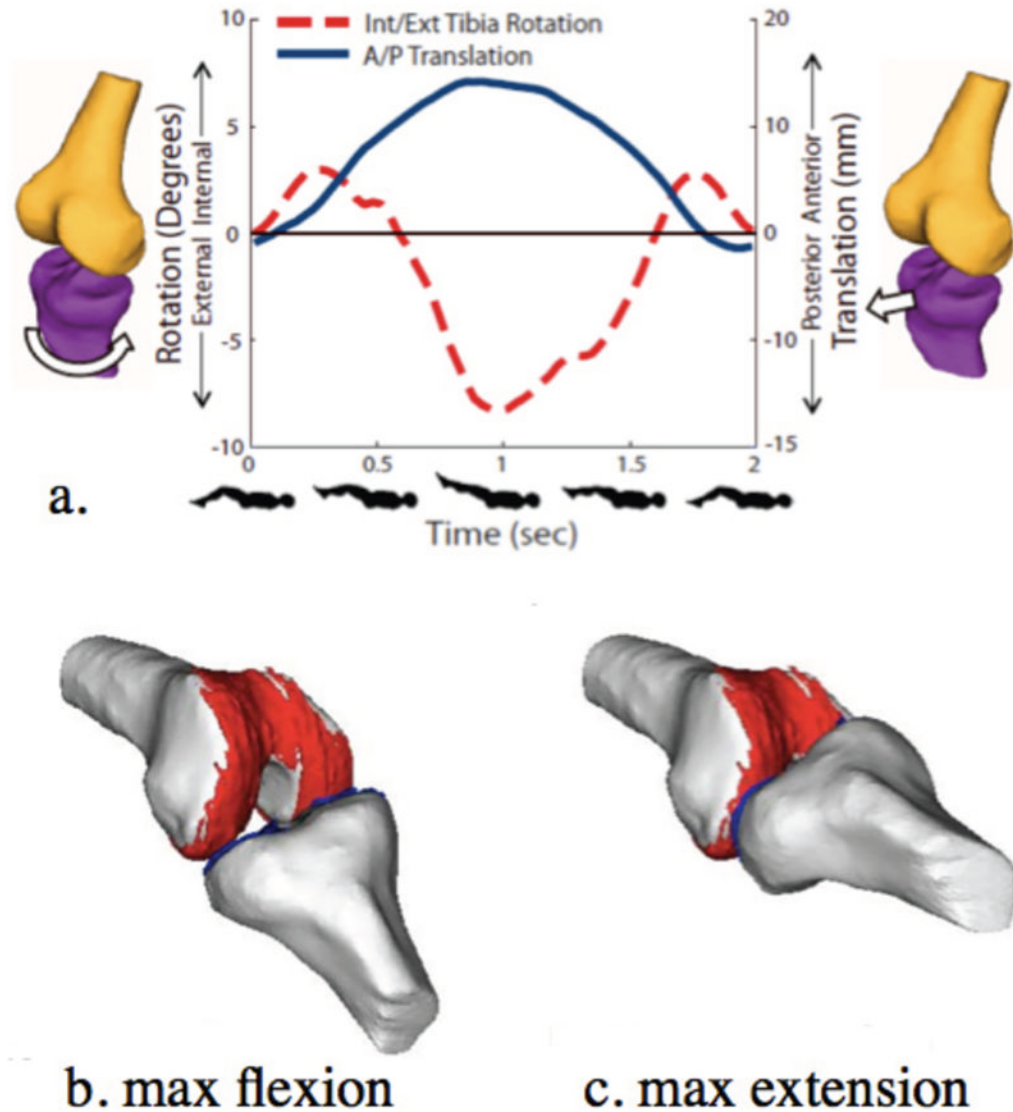


**Figure 3.**

3D joint kinematic data (a) and models (a,b,c) derived from Cine-PC MR images (TR/TE: 6.8/3.3 msec) of a healthy knee acquired in 5:36 minutes under a load similar to that of walking. External tibial rotation and anterior tibial translation can be visualized from extension to 37° of flexion (a) and when coupled with segmented bone and cartilage models, can be used to demonstrate contact and motion of the tibio-femoral joint throughout a cycle of flexion (b) and extension (c). (Reproduced from Bradford R, Johnson K, Wieben O and Thelen D. Dynamic imaging of 3d knee kinematics using PC-VIPR. In: Proceedings of the 19<sup>th</sup> Annual Meeting of ISMRM, Montréal, Québec, Canada, 2011 (Abstract 3178), with permission.)

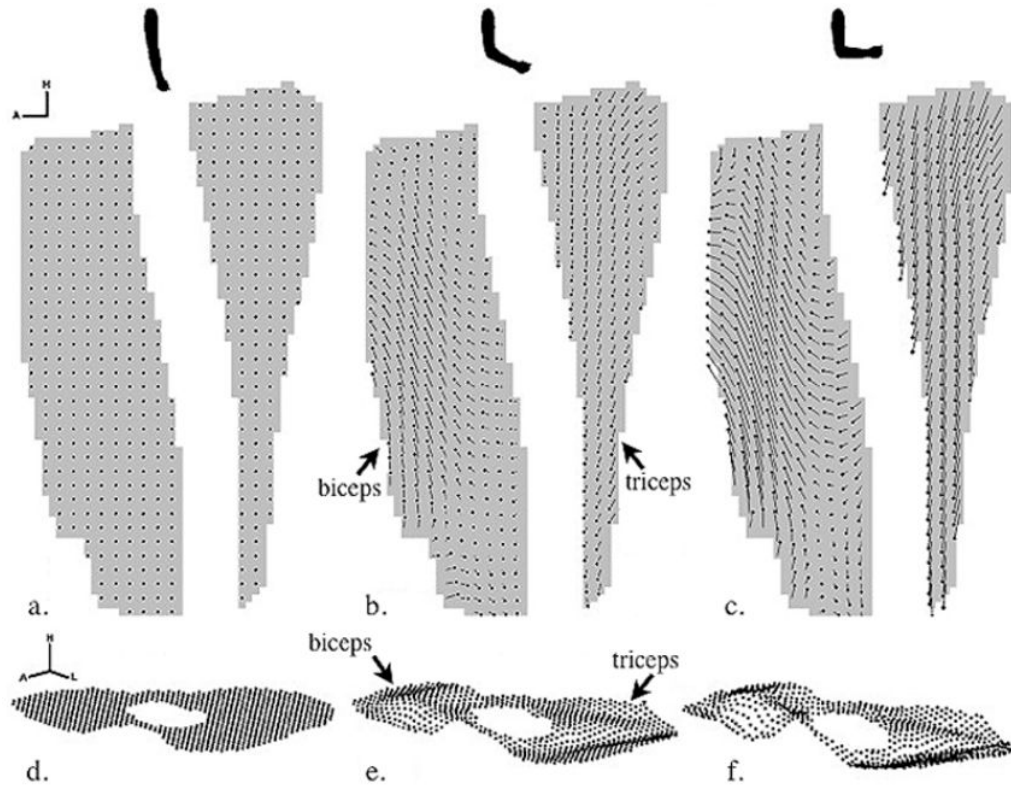


**Figure 4.**

Displacement maps of motion phases that correspond to elbow extension (**a, d**), approaching elbow flexion (**b, e**) and elbow flexion (**c, f**). Sagittal 2D displacement maps in which the head of the displacement trajectory indicates the 2D position of that element of muscle at this point in time and the tail indicates the position at the initial point in time (**a-c**). The 2D axis signifies the head and anterior directions. For visualization purposes, the displacement map is spatially under-sampled. Axial 3D displacement maps in which the dots indicate the 3D positions of that element of muscle at this point in time (**d-f**). The 3D axis signifies the head, left and anterior directions. Lastly, the displacement maps illustrate that the biceps and triceps muscle move antagonistically during elbow flexion. (Reproduced from Zhong X, Epstein FH, Spottiswoode BS, Helm PA, Blemker. *Imaging two-dimensional displacements and strains in skeletal muscle during joint motion by cine DENSE MR*, *J Biomech* 2008;41:532-40, with permission of Elsevier.)

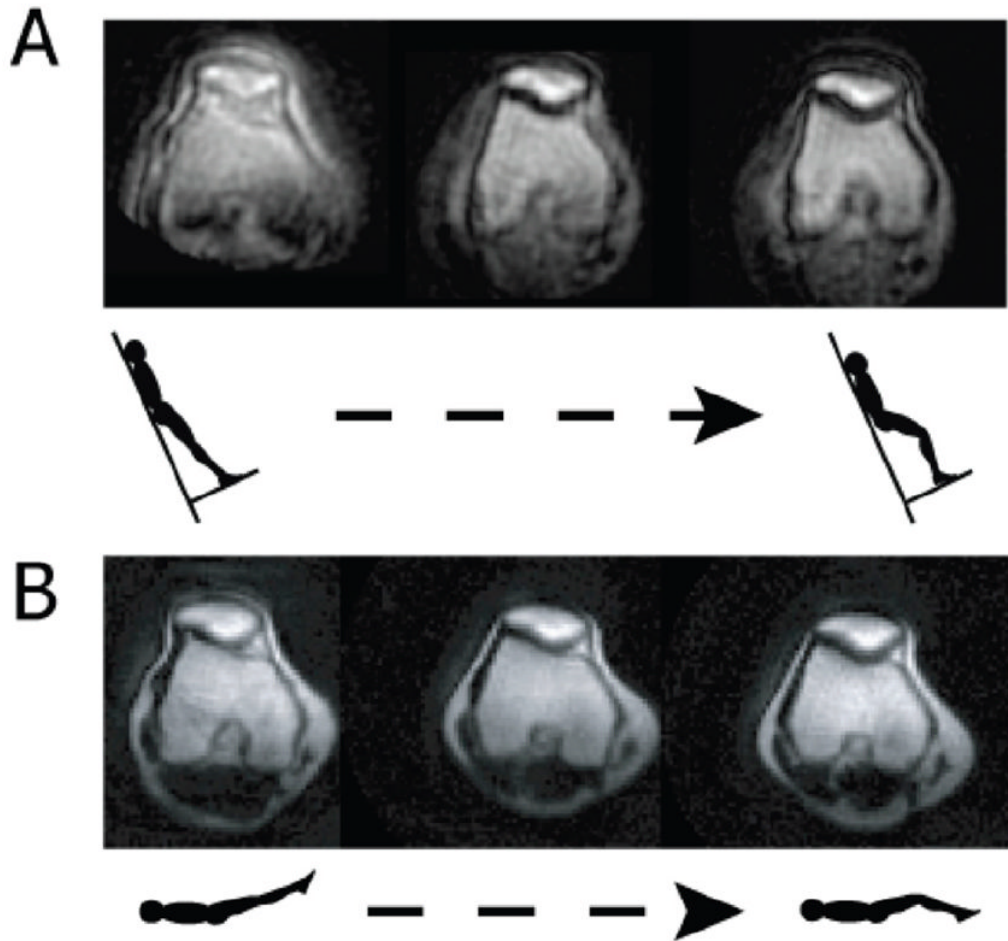


**Figure 5.**

Real-time MR images in the oblique axial plane through the widest portion of the patella during upright, weight-bearing knee extension at 0.5T and 90% of body weight (**a**) and supine, non-weight bearing knee extension at 1.5T (**b**) in a patellofemoral joint maltracker from knee flexion (30) to full extension. Differences between upright, weight bearing and supine, non-weight bearing MR imaging can be seen using real-time MRI. (Reproduced from Draper CE, Besier TF, Fredericson M, Santos JM, Beaupre GS, Delp SL, et al. Differences in patellofemoral kinematics between weight-bearing and non-weight-bearing conditions in patients with patellofemoral pain. *J Orthop Res* 2010;29:312-7, with permission of Wiley-Liss, Inc, a subsidiary of John Wiley & Sons, Inc.)

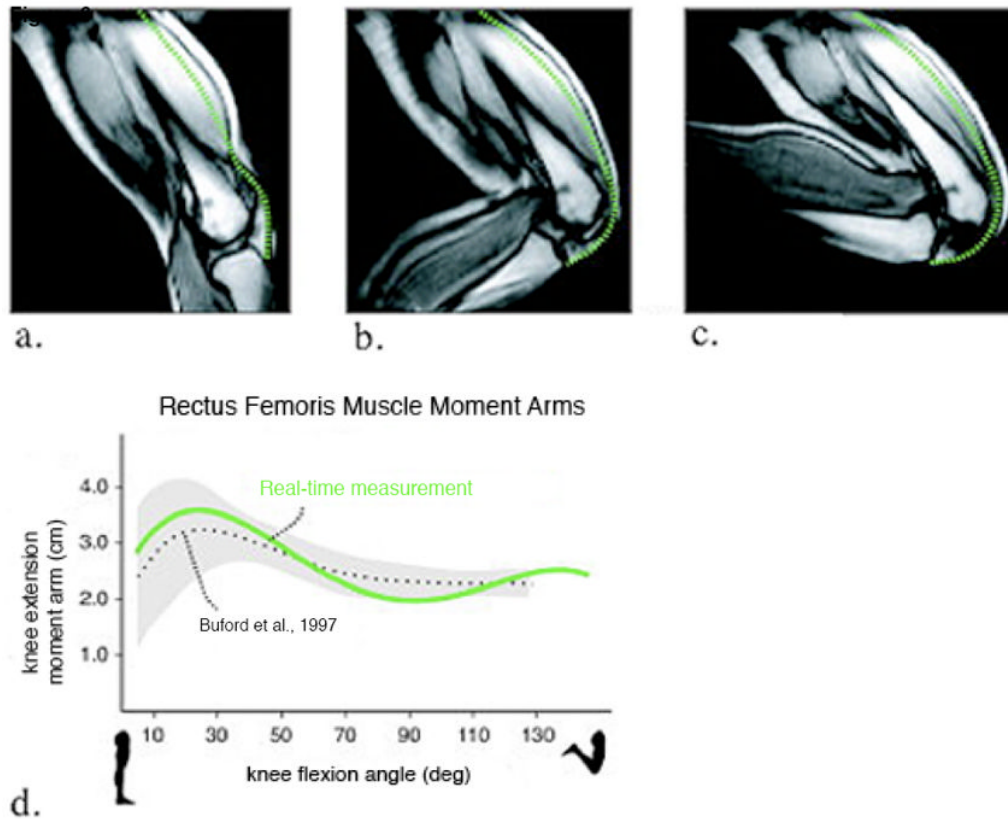


**Figure 6.**

Real-time MR images at frame 1 (**a**), frame 10 (**b**) and frame 20 (**c**) acquired during dynamic knee extension-flexion and used to calculate knee extension moment arms of the rectus femoris (**d**). Rectus femoris muscle-tension length measurements (**green dashed lines**) are shown in figures a-c. The knee joint angles for each frame were also measured and moment arms were calculated through the range of motion. The moment arms were compared with Buford WL Jr, et al. (72) (dotted lines correspond to the average values from 15 cadaveric specimens; added regions correspond to  $\pm 1$  SD). (Reproduced from Blemker SS and McVeigh ER, Real-time measurements of knee muscle moment arms during dynamic knee flexion-extension motion. In: Proceedings of the 14<sup>th</sup> Annual Meeting of ISMRM, Seattle, WA, USA, 2006 (Abstract 3619), with permission.)



**Table 1**

Advantages and drawbacks of open configuration MRI

<b>Advantages</b>	<b>Drawbacks</b>
Imaging in more physiologic conditions	Lower field strength
Decreased patient confinement	Increased exam time and cost
	Less clinically available
	Possibility of fatigue or pain due to pathological condition

**Table 2**

Advantages and drawbacks of supine closed-bore MRI

<b>Advantages</b>	<b>Drawbacks</b>
Higher field strength	Imaging in less physiologic conditions
Decreased exam time and cost	Increased patient confinement
More clinically available	Specialized hardware may be required for loading or stress

**Table 3**

“Application, Accuracy and Subject-repeatability by Dynamic MR Technique

Technique	Application	Accuracy* (in mm of in-plane translation)	Subject-repeatability** (in mm of superior inferior translation / ° of patellar tilt)
Stress MRI	Imaging of joints in atypical positions or under a load	0.30 (0.11) <sup>31, 32</sup>	0.81 (0.37) / 1.04 (0.35) <sup>32</sup>
Cine PC MRI	Imaging of anatomy and velocity during dynamic tasks	0.28 (0.22) <sup>31</sup>	0.73 (0.31) / 1.10 (0.35) <sup>31</sup>
Real Time MRI	Imaging of anatomy and velocity during dynamic tasks in a single motion cycle	2.0 <sup>11, 31</sup>	-- / 2.0 <sup>11, 21</sup>

\* Validated accuracy reported for patellofemoral joint as absolute average error or RMS error. The mean standard deviation is listed in parentheses. Sagittal plane was assumed for in-plane motion, worst error for all three motion direction planes listed if all were acquired.

\*\* Validated subject-repeatability reported for the patellofemoral joint as mean across subjects of the standard deviation across trials.